AMERICAN SOCIETY FOR MICROBIOLOGY | Journal of Virology

Molecular and Cellular Biology | Full-Length Text

Impaired glucocorticoid receptor function attenuates herpes simplex virus 1 production during explant-induced reactivation from latency in female mice

Kelly S. Harrison,[1] Nishani Wijesekera,[1] Anastasia G. J. Robinson,[2] Vanessa C. Santos,[1] Robert H. Oakley,[2] John A. Cidlowski,[2] Clinton Jones[1]

AUTHOR AFFILIATIONS See affiliation list on p. 16.

ABSTRACT Following acute infection, sensory neurons in trigeminal ganglia (TG) are important sites for the life-long latency of human alpha-herpes virus 1 (HSV-1). Acute or chronic stress in humans correlates with increased reactivation from latency, which can lead to recurrent HSV-1 disease, for example, herpes labialis, herpes stromal keratitis, and encephalitis. The glucocorticoid receptor (GR) and the synthetic corticosteroid dexamethasone stimulate key viral transcriptional cis-regulatory modules, viral replication, and explant-induced reactivation from latency. Conversely, a GR-specific antagonist impairs explant-induced reactivation and viral replication. Based on these observations, we hypothesize that GR transcriptional activity enhances reactivation from latency. To test this hypothesis, the HSV-1 latency-reactivation cycle was examined in mice containing a serine 229 to alanine mutation in GR (GR^{S229A}) because phosphorylation of GR serine 229 is crucial for GR-mediated transcription. Virus yields from cornea and conjunctiva of infected GR^{S229A} mice ceased before wild-type (wt) mice, consistent with reduced viral replication in kidney cells from GR^{S229A} mice. However, viral DNA levels in TG were not significantly different during latency and similar numbers of TG neurons express GR in GR^{S229A} and WT mice. Strikingly, HSV-1 viral titers during explant-induced reactivation were significantly reduced in female GR^{S229A} mice versus male GR^{S229A} mice or wt mice. The number of VP16 + TG neurons in female GR^{S229A} mice was significantly lower than in male GR^{S229A} or wt mice (males and females) during the early stages of explant-induced reactivation. Collectively, these studies revealed that GR phosphorylation of serine 229 is more important in GR^{S229A} female mice versus males during explant-induced reactivation from latency.

IMPORTANCE A correlation exists between stress and increased episodes of human alpha-herpes virus 1 reactivation from latency. Stress increases corticosteroid levels; consequently, the glucocorticoid receptor (GR) is activated. Recent studies concluded that a GR agonist, but not an antagonist, accelerates productive infection and reactivation from latency. Furthermore, GR and certain stress-induced transcription factors cooperatively transactivate promoters that drive the expression of infected cell protein 0 (ICP0), ICP4, and VP16. This study revealed female mice expressing a GR containing a serine to alanine mutation at position 229 (GR^{S229A}) shed significantly lower levels of infectious virus during explant-induced reactivation compared to male GR^{S229A} or wild-type parental C57BL/6 mice. Furthermore, female GR^{S229A} mice contained fewer VP16 + TG neurons compared to male GR^{S229A} mice or wild-type mice during the early stages of explant-induced reactivation from latency. Collectively, these studies revealed that GR transcriptional activity has female-specific effects, whereas male mice can compensate for the loss of GR transcriptional activation.

Editor Anna Ruth Cliffe, University of Virginia, Charlottesville, Virginia, USA

Address correspondence to Clinton Jones, clint.jones10@okstate.edu.

The authors declare no conflict of interest.

See the funding table on p. 16.

Received 22 August 2023
Accepted 24 August 2023

Published 12 October 2023

[This article was published on 12 October 2023 with Kelly S. Harrison's contributions missing from the "Author Contributions" section. The section was updated in the current version, posted on 31 October 2023.]

KEYWORDS HSV-1, latency, glucocorticoid receptor, reactivation from latency

Infection of craniofacial mucosal membranes with human alpha-herpes virus 1 (HSV-1) leads to life-long latency in sensory neurons within trigeminal ganglia (TG) and central nervous system (CNS), including brainstem (1–3). Infection can also lead to serious recurrent eye infections, including herpetic stromal keratitis (4, 5), which causes tissue destruction and can lead to blindness (6). Long-term oral acyclovir treatment only reduces HSK recurrences by 41% because most cases are due to reactivation from latency (7). Approximately, 400,000 individuals in the United States suffer from recurrent HSV-1 eye disease. Similarly, HSV-induced encephalitis is the most common cause of sporadic, fatal encephalitis, and two-thirds of all cases are the result of viral reactivation from latency (8–11).

Following acute infection where high levels of infectious virus are produced, HSV-1 establishes a life-long latent infection in neurons (12, 13). The HSV-1 latency-reactivation cycle is operationally divided into three distinct steps: establishment, maintenance, and reactivation. During the establishment of latency, a subset of infected neurons survive, viral gene expression is silenced, and latency is established (14). Maintenance of latency also requires survival of infected neurons, restricted lytic cycle viral gene expression, and little or no virus shedding. The only viral gene abundantly expressed in latently infected neurons is the latency-associated transcript (LAT) locus (15, 16). The LAT locus encodes six micro-RNAs, two novel small non-coding RNAs, a stable intron, three transcripts anti-sense to LAT (AL-1, AL-2, and AL-3) (17–19), and an upstream of LAT transcript. In general, LAT deletion mutants enhance reactivation from latency in rabbit and mouse models of infection (20). Notably, wild-type (wt) HSV-1, but not a LAT mutant, can undergo repeated heat-stress-induced reactivation events in a mouse model of infection indicating LAT is crucial for maintaining latency (21). LAT products impair apoptosis during the latency-reactivation cycle and in cultured cells (22–24) and productive infection (25). Collectively, LAT functions promote the establishment and maintenance of life-long latent infection in neurons.

Stress, physiological and psychological, is linked to an increased incidence of HSV-1 reactivation from latency in humans (26–28). Stress activates the hypothalamus-pituitary-adrenal axis, which stimulates the release of glucocorticoid hormones (GCs) (29). These hormones enter the cell, bind the glucocorticoid or mineralocorticoid receptors (GR, MR, respectively), enter the nucleus, bind specifically to GR response elements, and stimulate gene expression (30). The synthetic corticosteroid dexamethasone (DEX), which mimics the effects of endogenous corticosteroids, accelerates HSV-1 reactivation from latency (31). Approximately 50% of TG sensory neurons express GR (31, 32), thus it is plausible that corticosteroids and GR activation directly stimulate HSV-1 lytic cycle virus gene expression. GR and stress-induced transcription factors, Krüppel-like factor 4 (KLF4), KLF15, and Slug (Snai2) for example, cooperatively transactivate key immediate early (IE) viral promoters that drive the expression of transcriptional regulatory proteins, including infected cell protein 0 (ICP0) (33, 34), ICP4 (35), ICP27 (36), or VP16 (37). GR may also promote viral replication and spread by interacting with two transcription factors (AP-1 and NF-κB) that stimulate the expression of inflammatory cytokines and innate immune modulators: consequently, corticosteroids exhibit anti-inflammatory properties (38).

The objective of this study was to test whether GR regulates the HSV-1 latency-reactivation cycle using a mouse ocular infection model. A mouse strain that contains a serine to alanine mutation in position 229 of GR (GR^{S229A}) was used for these studies. These studies revealed virus production during explant-induced reactivation from latency is significantly reduced in female GR^{S229A} mice relative to male GR^{S229A} mice or parental wt C57BL/6J mice regardless of sex. Reduced virus shedding correlated with lower numbers of VP16 + TG neurons in female GR^{S229A} mice during early stages of explant-induced reactivation. These studies highlight the complexity of HSV-1-host interactions during early stages of reactivation from latency.

RESULTS

Analysis of GR^{S229A} mice and cells obtained from these mice

To test whether GR plays a role in the HSV-1 latency-reactivation cycle, a mutant mouse strain where the murine GR contains a serine 229 to alanine mutation (GR^{S229A}) was used. The mouse GR serine 229, and its human homolog GR serine 211, can be phosphorylated by several protein kinases, and phosphorylation is essential for optimal GR-mediated transcriptional activation, reviewed in reference (39). Mutation of serine 211 of the human GR induces conformational changes in the GR activation function region-1, which correlates with reduced transactivation of promoters containing GREs (40).

Although GR knockout mice were developed (41, 42), most pups die at birth because of respiratory failure (43). A conditional GR mutant that does not express GR in the nervous system (Gr^{NesCre}) was also developed (44); however, Gr^{NesCre} mice are smaller than parental mice and have altered fat deposition because they express higher levels of corticosteroids in serum due to disruption of the hypothalamic/pituitary axis. Thus, this strain did not appear to be suitable for the goals of this study. Conversely, GR^{S229A} breed efficiently, pups are healthy, and similar numbers of male and female pups are born. Genotyping of mice confirmed male and female GR^{S229A} breeding pairs contained the ~230 bp mutant GR^{S229A} fragment flanked by double-mutant Lox71/Lox66 and Lox2272 sites: conversely, the same primers yielded a smaller ~180 bp fragment in parental C57BL/6J mice (Fig. 1A).

Primary kidney cells were prepared from GR^{S229A} mutants and parental C57BL/6J mice (referred to as wt mice hereafter) to compare GR phosphorylation at Ser 229. Kidney cells were used for these initial studies because they have a relatively high rate of proliferation and do not senesce as rapidly as primary cells derived from other organs. An antibody that specifically recognizes phosphorylated GR on serine 211/229 was used for this study. Upon addition of DEX, phosphorylated GR (Phos-GR) localized to the nucleus of wt mice, which was expected (39, 45) (Fig. 1B). Conversely, Phos-GR staining in kidney cells derived from GR^{S229A} mice was not detected after DEX treatment (Fig. 1B). As expected, a monoclonal antibody that recognizes total GR revealed strong fluorescence in wt and GR^{S229A} mice (Fig. 1C).

To further confirm the loss of serine 229 phosphorylation in GR^{S229A} mutant mice, western blots using antibodies that recognize total GR or phosphorylated GR were performed (Fig. 1D and E). Wt or GR^{S229A} mice were treated with DEX (1 mg/kg of body weight) for 2 h to stimulate GR phosphorylation prior to the collection of lung tissue. Mice treated for 2 h with vehicle (PBS) served as controls. Phosphorylated GR was detected in wt animals treated with PBS, and DEX treatment resulted in enhanced phosphorylation (Fig. 1D and E). As expected, the antibody that specifically recognizes phosphorylated GR on serine 211/229 did not detect GR in GR^{S229A} mice regardless of whether DEX was added. Total GR was readily detected in wt and GR^{S229A} regardless of DEX treatment.

Examination of HSV-1 replication in primary kidney cells from GR^{S229A} mice

Primary kidney cells from GR^{S229A} or wt mice were subsequently infected with the neurovirulent HSV-1 strain McKrae at a multiplicity of infection (MOI) of 1. Twenty-four hours after infection virus replication was measured by plaque assays (Fig. 2). Male and female wt kidney cells yielded ~7 × 10^3 PFU/mL. In sharp contrast, kidney cells derived from GR^{S229A} males and females shed significantly lower levels of infectious virus (~3 × 10^3 PFU/mL). These studies indicated that GR phosphorylation of Ser 229 enhances viral replication in primary kidney cells, which is consistent with previous studies demonstrating a GR-specific antagonist CORT-108297 significantly reduced viral replication in a mouse neuroblastoma cell line (Neuro-2A) (33).

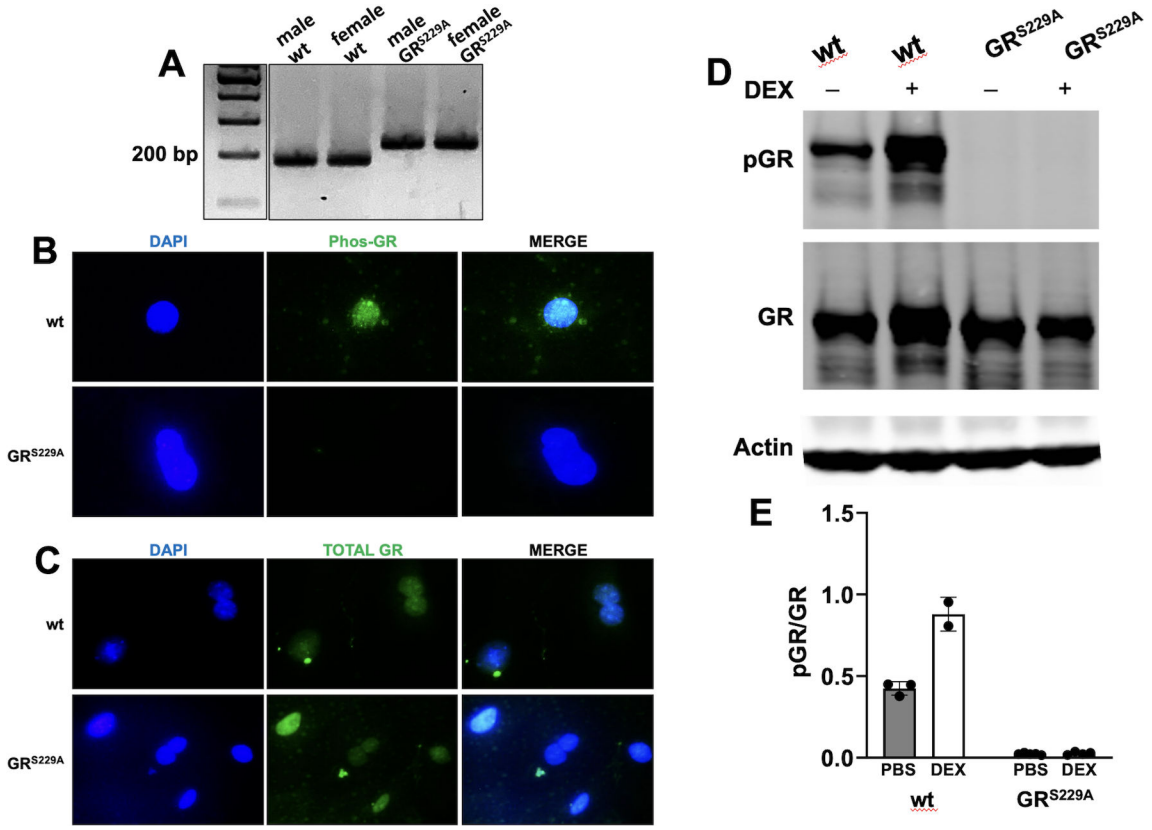

FIG 1 Confirmation GR^{S229A} mice do not express phosphorylated serine 229. (A) Representative PCR genotyping of wt and GR^{S229A} male and female mice. WT mice display bands at 180 bp using primers described in Materials and Methods. Conversely, the same primers amplify a 230 bp fragment in GR^{S229A} mice confirming the flanking Lox sites are present. (B and C) Primary kidney cells from wt or GR^{S229A} male or female mice (n = 5 mice/group, two independent experiments) were prepared. These cells were treated with DEX and stained for serine 229 phosphorylated GR (panel B, green) or total GR (panel C, green). DAPI nuclear staining (blue) was included in all samples to visualize GR nuclear localization. Representative images from female mice are shown (40× magnification). (D) Representative western blot from wt and GR^{S229A} animals. Mice were treated with vehicle (PBS) or DEX for 2 h prior to tissue collection. Membranes were probed with antibodies specific for phosphorylated GR (pGR) or total GR. β-actin was included as a loading control. (E) Quantification of phosphorylated GR to total GR from western blots. Data represent the mean ± SD (n = 2–5 mice per group).

Comparison of HSV-1 titers during acute infection in wt mice versus GR^{S229A} mutant mice

Virus replication during acute infection in GR^{S229A} mutant mice was compared to wt mice. Eight-week-old male and female mice were ocularly infected with HSV-1. Ocular swabs were collected every other day for 10 days, and then every 5 days (Fig. 3A). Plaque assays were used to measure virus titers from the cornea and conjunctiva. Male and female wt control animals and GR^{S229A} female mice shed similar levels of virus (10^4–10^5 PFU/mL) at 2- and 4 days post-infection (dpi) (Fig. 3B). However, GR^{S229A} males shed significantly lower levels of infectious virus, never reaching above 10^4 PFU/mL (Fig. 3B). Male and female GR^{S229A} mice stopped shedding virus from cornea and conjunctiva at 6 dpi; however, wt males and females shed virus until 8 dpi. From 10 dpi until 30 dpi, infectious virus was not detected in ocular swabs indicating latency was established and maintained.

Since TG are an important site for HSV-1 latency after ocular infection (46), virus replication was measured in TG at 4 and 8 dpi. At 4 dpi, wt and GR^{S229A} mice were shedding ~5×10^3 PFU/mL infectious virus in TG (Fig. 4A). At 8 dpi, TG from wt male or female mice were shedding ~10^3 PFU/mL infectious virus. In contrast, virus was not detected in TG of GR^{S229A} mice at 8 dpi (males and females; Fig. 4A).

To assess viral DNA levels in TG, qPCR was performed using primers directed against the HSV-1 glycoprotein B (gB) gene, which is highly conserved across all HSV-1 strains

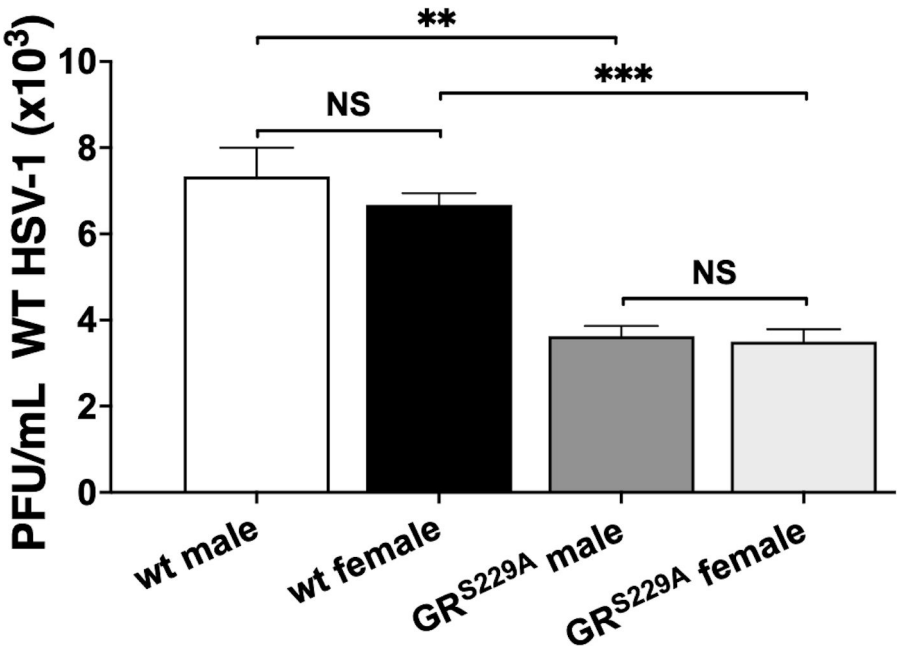

FIG 2 HSV-1 infection of primary kidney cells. Primary kidney cells were prepared from wt and GR^{S229A} mice (males and females: n = 4–6 from three separate experiments). These cells were infected with HSV-1 at an MOI of 1. Twenty-four hours post-infection cells were collected, freeze-thawed three times at 37°C/−80°C, and used to plaque on Vero cell monolayers. Data shown are the mean ± SD for triplicate wells of duplicate experiments in PFU/mL × 10^3. NS is not significant; $^{**}P < 0.01$ and $^{***}P < 0.005$ by Student's t-test.

(47–49). Female GR^{S229A} had significantly lower levels of gB DNA relative to GAPDH DNA in TG at 4 dpi (Fig. 4B). Male GR^{S229A} had slightly elevated gB DNA levels; however, these differences were not statistically significant relative to wt mice at 4 dpi. By 8 days post-infection and latency (30 dpi), gB DNA levels were 2-log lower than 4 dpi (Fig. 4C and D). No significant differences in gB DNA levels were identified in any of the groups at 8 or 30 dpi suggesting establishment of latency was not significantly different in wt versus GR^{S229A} mice (Fig. 4C).

Total GR expression is similar in wt mice and GR^{S229A} mice during acute infection and latency

Immunohistochemistry studies were performed to compare the number of TG neurons expressing GR in wt versus GR^{S229A} mice during acute infection (4 dpi) or latency (denoted as L in Fig. 5 and 6). TG from mice at 4 dpi (Fig. 5A) and 30 dpi (Fig. 5B) were dissected and immunohistochemistry (IHC) studies were performed. Since virus shedding is not readily detected at 30 dpi (Fig. 2B), this time-point is operationally defined as latency. There was not a significant difference in the number of TG neurons expressing total GR in GR^{S229A} mice versus wt mice during acute infection or latency (Fig. 5C). Approximately 50% of TG neurons expressed GR, consistent with independent studies (31, 32).

Additional studies compared GR phosphorylation in TG neurons at 4 dpi or 30 dpi (latency). Two important observations were observed: (i) GR phosphorylation of serine 229 was readily detected in TG neurons of wt mice but not GR^{S229A} mice at 4 dpi (Fig. 6A); and (ii) GR phosphorylation of serine 229 was not readily detected in TG neurons during latency for all mice (Fig. 6B). Quantification of TG neurons stained with the GR antibody that specifically recognizes serine 229 confirmed wt mice contained significantly more TG neurons when stained at 4 dpi (Fig. 6C). In summary, these studies revealed that GR^{S229A} mice expressed similar levels of GR in TG neurons, but serine 229 phosphorylation was not detected in GR^{S229A} mice, consistent with the studies presented in Fig. 1.

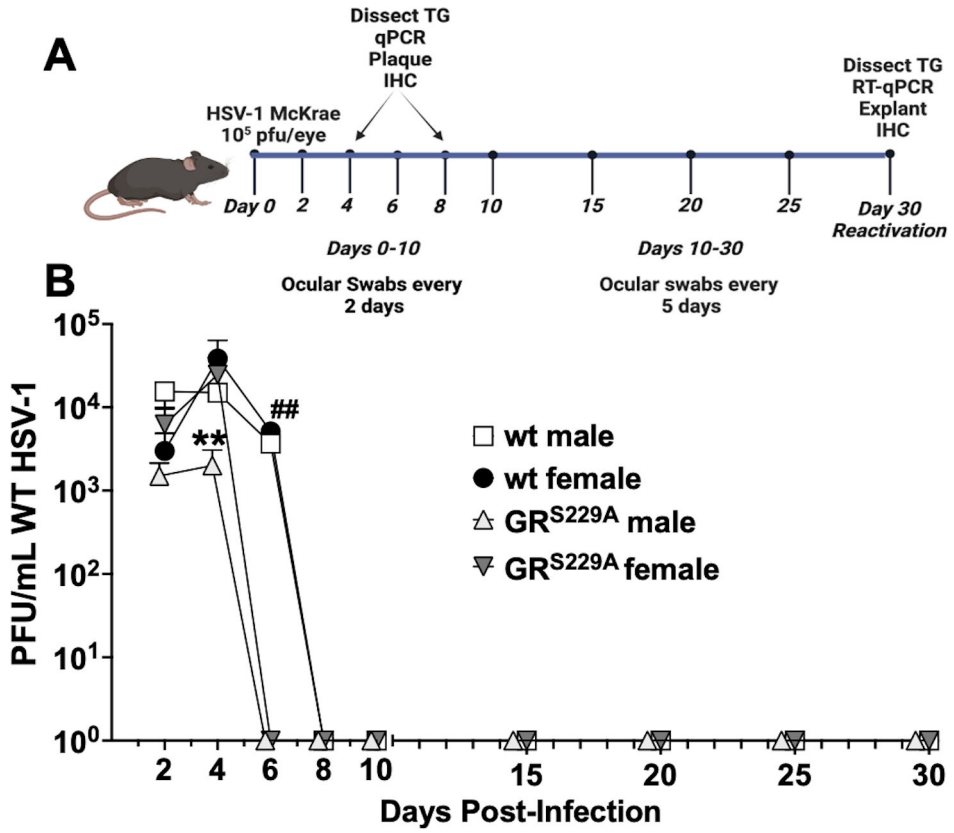

FIG 3 Examination of HSV-1 ocular shedding in GR^{S229A} or wt mice. (A) Schematic of animal infection studies. GR^{S229A} or wt mice were ocularly infected with HSV-1 on day 0. Every other day, ocular swabs were collected until day 10 when swabs were then collected every 5 days. On days 4, 8, and 30, mice were humanely euthanized, and TG dissected. (B) Infectious virus in ocular swabs was measured at the denoted days after infection for each group. Data are shown as timeplot mean ± SEM of individual animals (n = 5 mice/group, three separate experiments); **P < 0.01 t-test as compared to every other group; ## P < 0.01 for wt mice compared to GR^{S229A} mice using unpaired t-test.

Explant-induced reactivation from latency is impaired in GR^{S229A} female mice

TG from latently infected mice (30 dpi) were dissected, minced into smaller pieces, and incubated with minimal essential medium (MEM) + 2% charcoal-stripped fetal bovine serum (FBS) in the presence of DEX to accelerate virus reactivation (31). FBS that is passed through a column containing "activated" charcoal will remove hormones, lipid-based molecules, certain growth factors, and cytokines yielding stripped FBS. However, this process does not remove salts, glucose, and most amino acids. Aliquots of supernatant were collected to measure the shedding of infectious virus (Fig. 7). Notably, GR^{S229A} female mice shed significantly lower levels of virus at every timepoint examined relative to wt mice or male GR^{S229A} mice. For example, virus shedding from female GR^{S229A} mice did not exceed 10^3 PFU/mL. Conversely, TG from wt male and female mice, and GR^{S229A} males, shed higher levels of infectious virus in a time-dependent manner after explant, which is consistent with previously published studies (31, 50). Viral titers from wt mice (males and females) and GR^{S229A} males increased from approximately 10^4 PFU/mL at 6 days after explant to approximately 10^6 PFU/mL at 10 days after explant.

LAT expression is reduced in TG of GR^{S229A} female mice

LAT expression is a hallmark of latency because it is the only viral transcript abundantly expressed during latency, reviewed in references (13–16). TG from latently infected mice were used to prepare total RNA and perform reverse transcription and quantitative polymerase chain reaction (RT-qPCR) to detect LAT expression. Surprisingly, significantly

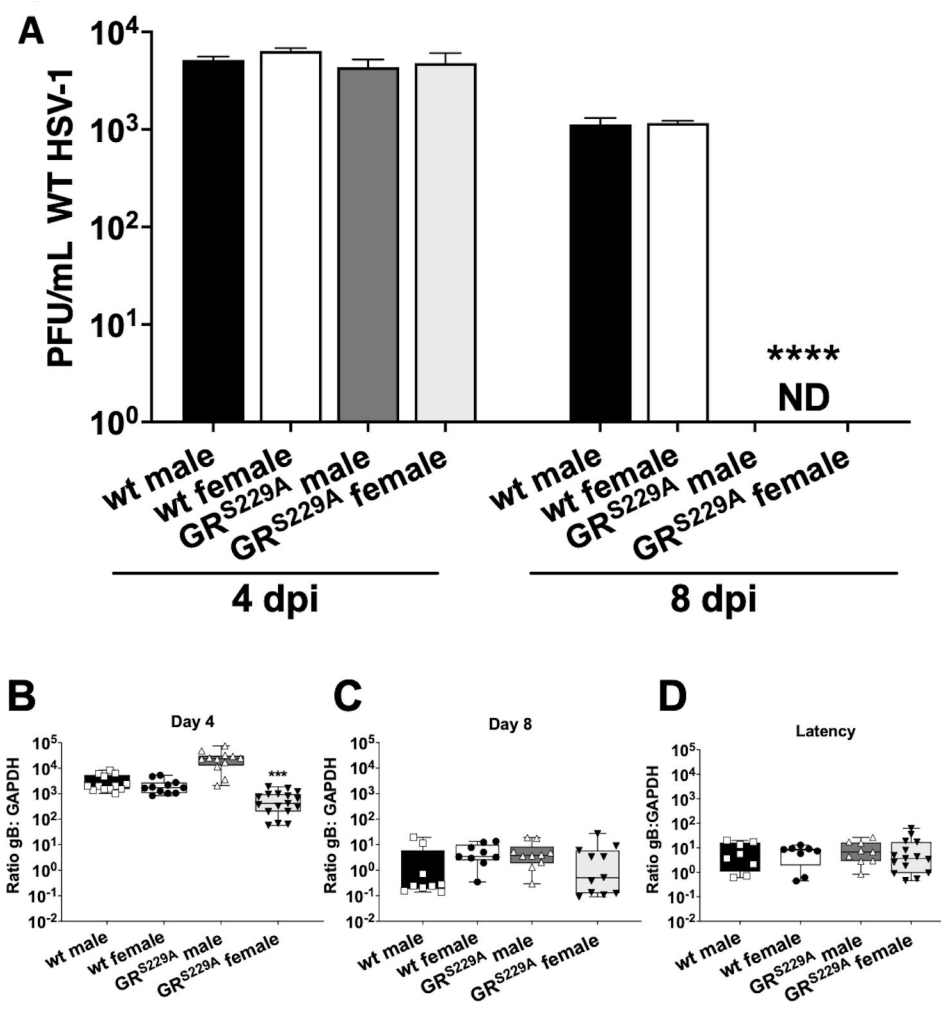

FIG 4 Measurement of infectious virus in mouse TG during acute infection. (A) TG were dissected from animals at 4 and 8 days post-infection, TG were collected, minced into three to four pieces, and then incubated with Vero cell monolayers to plaque for HSV-1. ND: none detected. (B–D) At 4-, 8-, and 30 days post-infection (latency), TG were collected from four animals/group. DNA was prepared from the respective samples, and qPCR was performed using gB primers for HSV-1 or mouse GAPDH DNA. Ratio of gB:GAPDH DNA was calculated using the Delta-Delta CT method. Left and right TG were analyzed separately. ***$P < 0.005$ using Student's *t*-test. For these studies, $n = 4–6$ mice/group, and two separate experiments were performed.

lower levels of LAT were observed in TG from GR^{S229A} female mice relative to wt mice (males or females) (Fig. 8). This was unexpected because viral DNA levels were similar in wt and GR^{S229A} mice regardless of sex (Fig. 4D). To further confirm decreased levels of LAT expression, the ratio of LAT to viral genomes was calculated. As observed in Fig. 8A and 4D, the ratio of LAT to gB is consistent for wt and GR^{S229A} male animals with ~10× more LAT expression than gB (Fig. 8B). In comparison, GR^{S229A} female mice expressed significantly lower LAT:gB ratio, with 10× more gB DNA compared to LAT RNA levels.

In summary, these studies revealed that female GR^{S229A} mice produced lower levels of infectious virus during explant-induced reactivation from latency, which correlated with reduced LAT expression in female GR^{S229A} mice.

Examination of ICP0, ICP4, and VP16 in TG neurons during early stages of explant-induced reactivation from latency

We suggest the efficiency of reactivation from latency is regulated by at least three distinct steps: (i) the number of neurons that express lytic cycle genes and produce

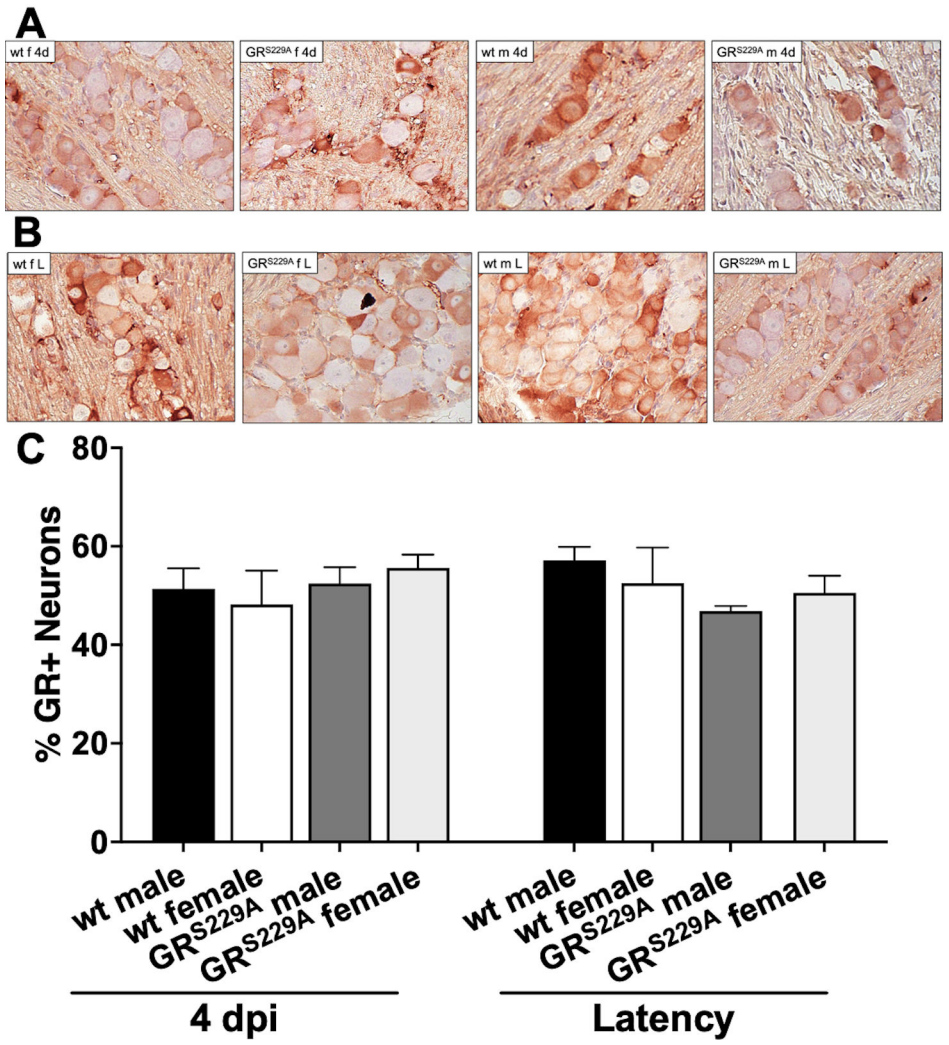

FIG 5 GR expression in TG of HSV-1 infected mice. (A) Representative IHC images of total GR expression in TG from wt or GR^{S229A} mice (males and females) at 4 dpi. Female mice are denoted (F), males (M), 4 days (4 dpi), or L (latency) (n = 4–6 mice/group, two independent experiments). (B) IHC of total GR expression in TG from male (M) and female (F), wt or GR^{S229A} mice (n = 5 mice/group, three separate experiments). (C) Quantification of GR-positive TG neurons from IHC in panels A and B. Data are shown as percentage of GR-positive TG neurons out of 500 total TG neurons counted per field of view.

infectious virus following the initial "reactivation stimulus," (ii) secondary spread of infectious virus to adjacent neurons plus perhaps non-neuronal cells, and (iii) efficiency of lytic cycle viral gene expression in cells after secondary virus spread and subsequent production of infectious virus. To examine the expression of key viral regulatory proteins in TG neurons during early stages of explant-induced reactivation, IHC was performed as previously described (31, 37). For these studies, we examined ICP0, ICP4, and VP16 expression in TG neurons. The rational for choosing these three viral proteins is they have been reported to trigger reactivation from latency, reviewed in reference (12). TG were dissected and incubated with 2% stripped FBS and DEX for 8 h prior to formalin fixation, paraffin embedding, and IHC. Eight hours after TG explant was chosen because previous studies demonstrated ICP0, ICP4, and VP16 can be detected in TG neurons by IHC (31). However, ICP0, ICP4, and VP16 protein expression are not readily detected in TG neurons at 4 h after explant (31). Based on these observations, secondary spread of infectious virus and subsequent expression of viral genes in adjacent neurons or non-neuronal cells is not likely to occur at 8 h after TG explant. Fewer VP16 + TG neurons were detected in GR^{S229A} females when compared to wt mice (females and males) and GR^{S229A} males 8 h

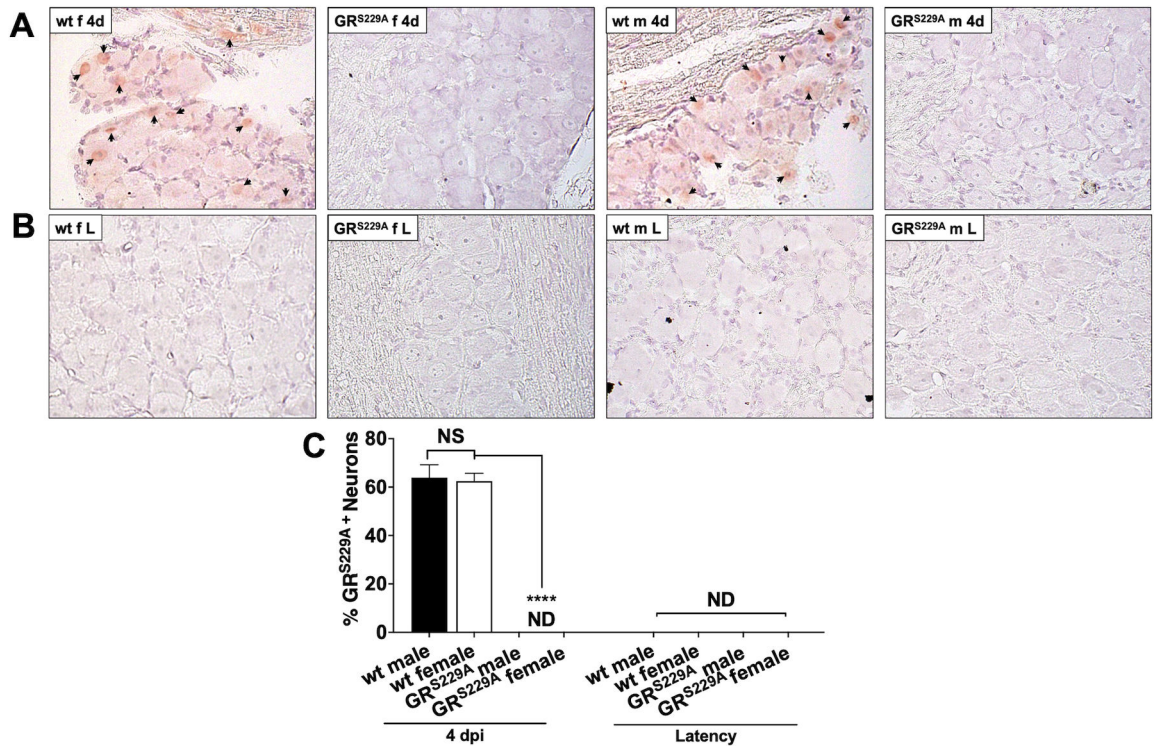

FIG 6 Examination of phosphorylated GR in TG of HSV-1 infected mice. (A) IHC of GR serine 229 phosphorylation from wt or GR^{S229A} male (M) and female (F) mice infected with HSV-1 for 4 days (n = 4–6 mice/group, two independent experiments). Black arrows denote positively stained TG neurons. (B) GR^{S229A} IHC in male (M) and female (F), wt and GR^{S229A} mice (n = 5 mice/group, three separate experiments) 30 days post-infection (latency, "L"). (C) Data derived from IHC studies in panels A and B were quantified. Results are shown as percentage of positive phosphorylated-GR neurons out of 500 counted neurons per field of view. NS: not significant; ND: none detected; ****P < 0.001 Student's t-test.

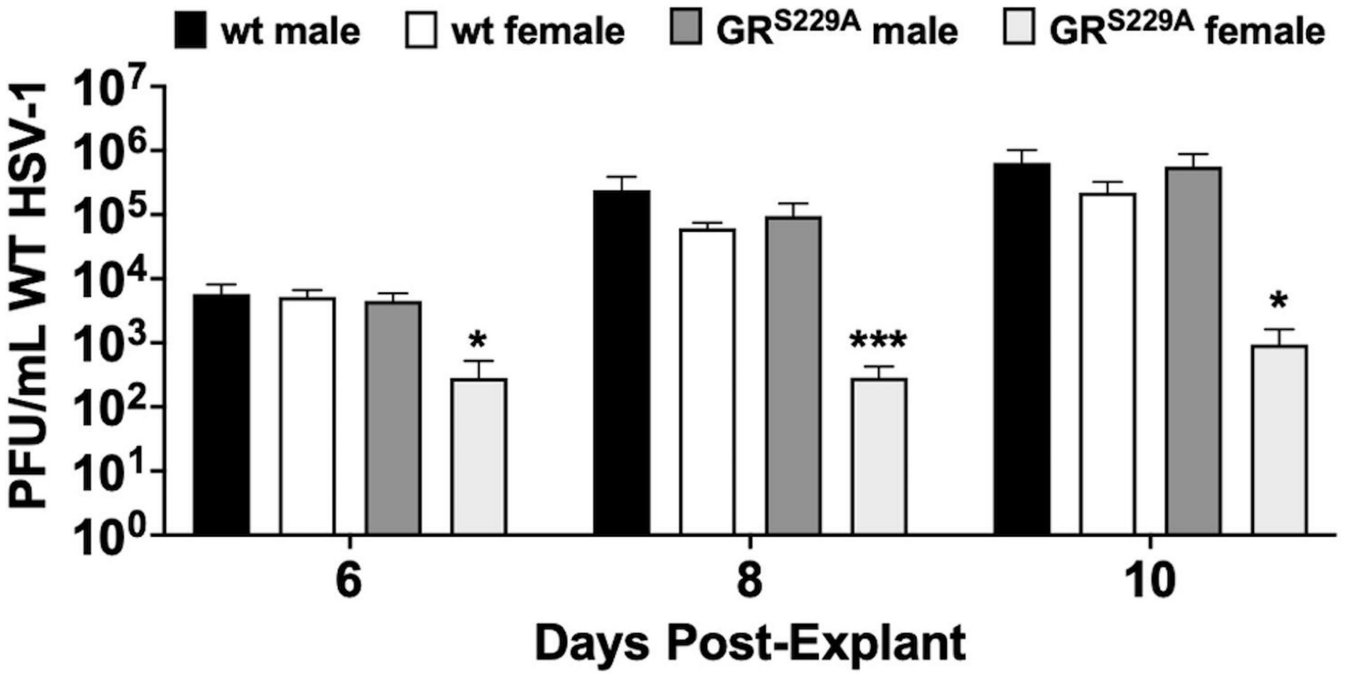

FIG 7 Examination of HSV-1 explant-induced reactivation. TG from male or female wt and GR^{S229A} mice were dissected 30 dpi (latency) (n = 5 mice/group and three independent experiments). After mincing TG into small pieces, pieces were incubated in MEM + 2% stripped FBS and 10 µM DEX. Daily aliquots of MEM were collected and used to measure virus titers during HSV-1 explant-induced reactivation from latency; *P < 0.05 and ***P < 0.005 by Student's t-test.

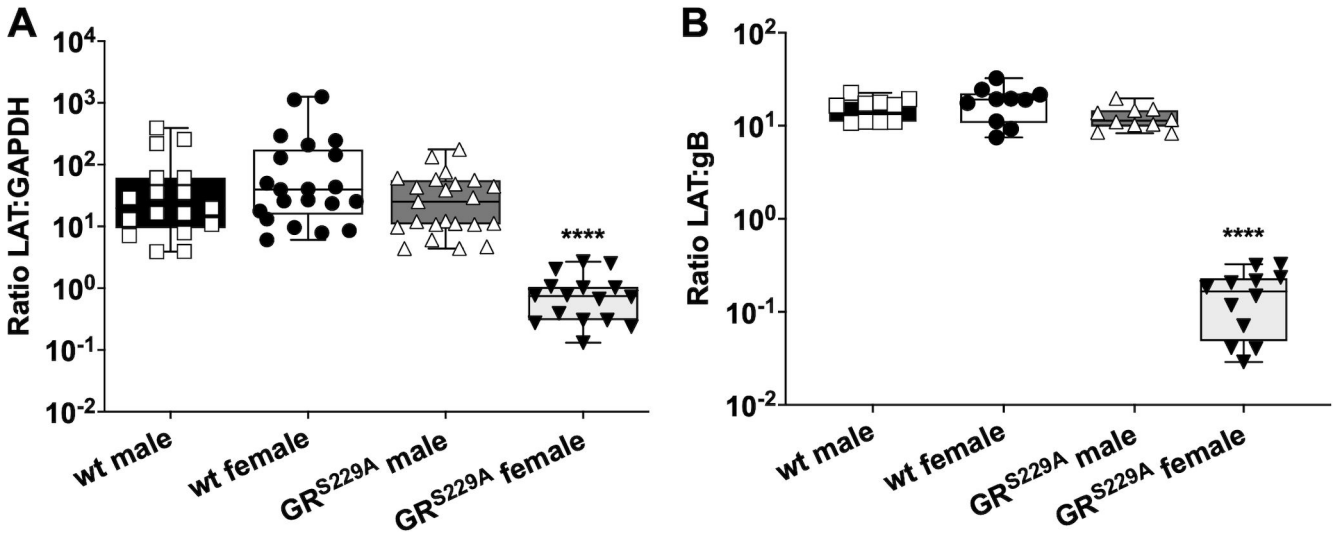

FIG 8 LAT expression in TG of latently infected mice. (A) TG from latently infected mice (30 dpi) were dissected from five mice/group from three separate experiments and then incubated in TRIzol. RNA was prepared as described in Materials and Methods. cDNA was synthesized using random hexamers, and qPCR was performed using primers for HSV-1 LAT and mouse GAPDH. Data are shown as the ratio of LAT:GAPDH RNA. Left and right TG from each animal were analyzed separately: ****$P < 0.001$ using Student's *t*-test. (B) RT-qPCR Cq values for LAT expression were compared to Cq values from qPCR for gB DNA to calculate the ratio of LAT expression to viral genomes. Data are shown as box plots from maximum to mininum values with a line at the median for two separate experiments ($n = 4$ mice each). ****$P < 0.001$ using Student's *t*-test.

after TG were explanted (Fig. 9A). Quantification of VP16 + TG neurons confirmed significantly fewer VP16 + TG neurons were detected in GR^{S229A} female mice (Fig. 9D). For all the mice, the number of TG neurons expressing ICP0 (Fig. 9B) was approximately 10% (Fig. 9D). Interestingly, the number of ICP4 + TG neurons (Fig. 9C) detected in the TG of GR^{S229A} female mice was higher relative to the other three groups (Fig. 9D). As previously reported (31), the number of VP16 + TG neurons at 8 h after explant-induced reactivation was higher than TG neurons expressing ICP0 or ICP4.

DISCUSSION

Increased episodes of reactivation from latency in people correlate with increased ultraviolet (UV) light exposure, heat stress (fever), trauma, immune suppression, and stress (12–14, 26, 28, 51, 52). Notably, these stimuli increase the incidence of reactivation from latency in mouse models of infection and/or stimulate productive infection in cultured cells (31, 52–54). These cellular stressors increase corticosteroid levels and presumably activate GR. For example, UVB and UVC, but not UVA, increase cortisol production in human skin cultures (55), and a single dose of UVB light treatment stimulates corticosteroid production in C57BL/6 mice (56). Furthermore, heat-stress-induced HSV-1 reactivation from latency is impaired by cyanoketone, an inhibitor of glucocorticoid synthesis (57). The phosphatidylinositol 3-kinase (PI3-kinase)/Akt signaling axis plays a pivotal role in maintaining HSV-1 latency in several rodent neuronal models of latency, reviewed in references (12, 57, 58). GR interacts with PI3-kinase (59) and inhibits PI3-kinase signaling (60). While these observations support a significant role for GR activation during reactivation from latency, certain latently infected neurons may have different pathways to reactivation that do not require increased corticosteroids or GR activation.

Infectious virus in cornea and conjunctiva of GR^{S229A} male and female mice ended 6 days after infection; however, high levels of infectious virus were detected in wt mice 6 days after infection. Reduced viral titers were also detected in primary kidney cells from GR^{S229A} male and female relative to primary kidney cells from wt mice. These observations suggest that reduced efficiency of lytic virus spread in TG may impair virus shedding

during explant-induced reactivation from latency in GR^{S229A} females. Since reduced viral titers were detected in GR^{S229A} males and females during acute infection and in primary kidney cells from GR^{S229A} males and females, other factors must mediate the female-specific reduction of virus shedding in GR^{S229A} mice during explant-induced reactivation. For example, the finding that fewer VP16 + TG neurons were detected in female GR^{S229A} mice

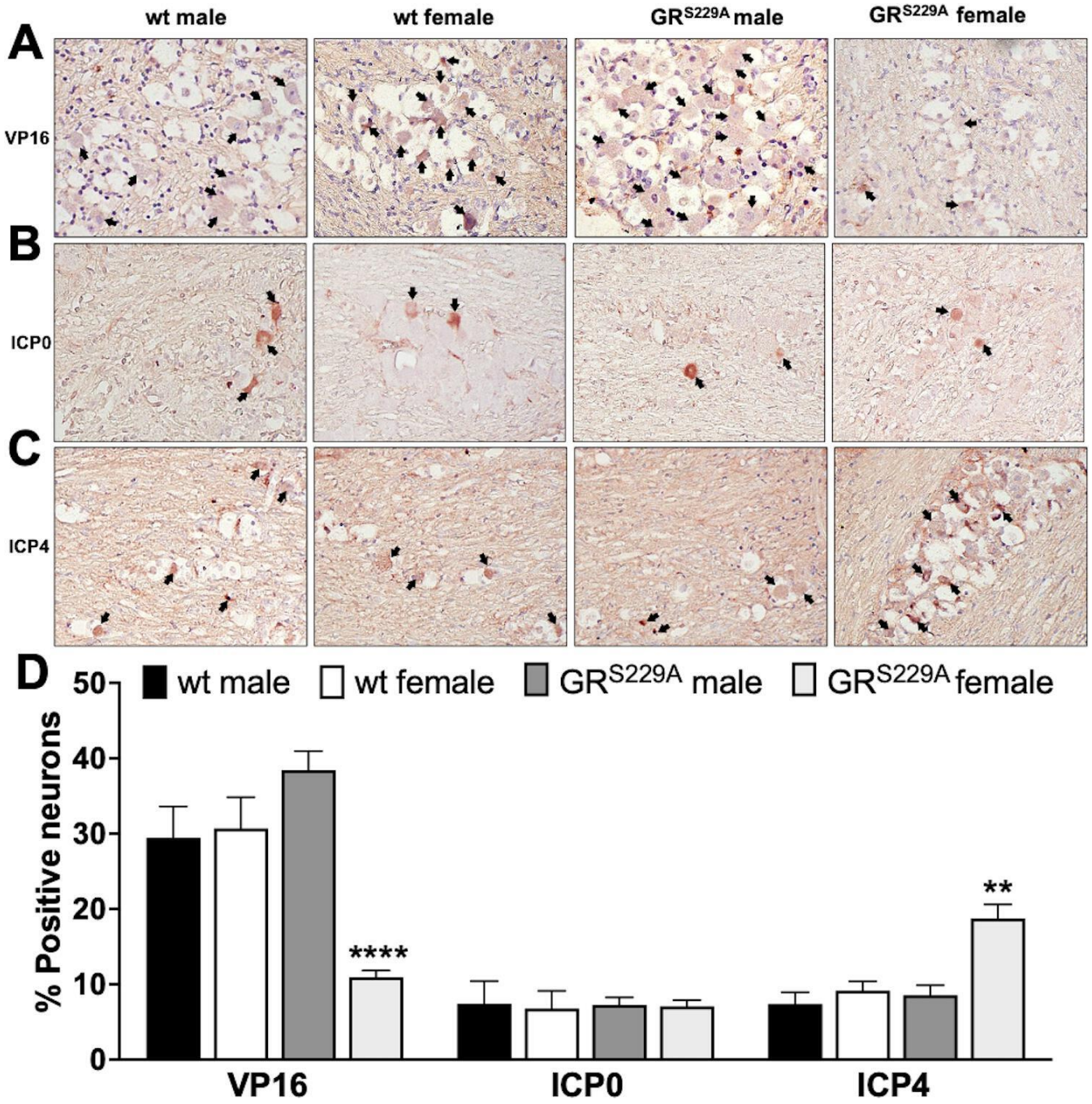

FIG 9 HSV-1 protein expression during reactivation from latency. TG from wt or GR^{S229A} male (M) and female (F) mice latently infected with HSV-1 (30 dpi) were collected and explanted in MEM + 2% stripped FBS and 10 µM DEX for 8 h. Tissues were then formalin fixed, paraffin embedded, and thin sections on glass slides stained with commercially available antibodies directed against VP16 (1:100, panel A), ICP0 (1:100, panel B), or ICP4 (1:200, panel C). Black arrows denote positively stained TG neurons. Data are shown as representative images from two separate experiments. (D) Quantification of key viral regulatory proteins during explant-induced reactivation. The percentage of positive TG neurons was calculated from TG sections shown in Fig. 9. A ratio of positively staining neurons to total neurons per field of view for a total of minimum 500 neurons. $^{**}P < 0.01$ and $^{****}P < 0.001$ using Student's *t*-test.

is predicted to be an important reason why reduced virus shedding occurred during explant-induced reactivation. Conversely, higher numbers of ICP4 + TG neurons in female GR^{S229A} mice do not correlate with reduced explant-induced reactivation. We also suggest additional cellular and viral factors negatively reduce virus shedding in GR^{S229A} females, but not males, during explant-induced reactivation.

Our studies also suggest sex-specific virus-host interactions in TG neurons mediate differences in viral titers of male versus female GR^{S229A} mice during explant-induced reactivation. Sex-specific differentially expressed genes (DEGs) were identified in TG neurons of C57BL/6 J mice using RNA-sequencing approaches (61). For example, female selective DEGs regulate (i) growth factors and their receptors; (ii) immune regulators; (iii) channel and transmembrane proteins that regulate nervous system function/development; and (iv) extracellular matrix proteins. Conversely, male selective DEGs were identified, which regulate: (i) oxidation–reduction, (ii) cellular respiration, and (iii) macromolecule and protein metabolism. This study also identified female-specific DEGs in TG, which regulate gene expression and translation. The male sex hormone, androgen, was also reported to regulate GR activity in a tissue-specific manner (62) suggesting androgen and the androgen receptor may enhance explant-induced reactivation in TG of male GR^{S229A} mice. Future studies are designed to examine the role the sex hormones (androgen, estrogen, and progesterone) and their respective receptors play during explant-induced reactivation from latency in wt and GR^{S229A} mice.

The HSV-1 genome contains numerous consensus GREs (C. Jones, unpublished data), but promoters that drive the expression of IE viral transcriptional regulators (ICP0, ICP4, or ICP27) do not contain consensus GREs. Despite lacking GREs, cis-regulatory modules (CRMs) in these promoters are transactivated by GR and certain stress-induced transcription factors (33–37). For example, GR and Krüppel-like factor 4 (KLF4) and KLF15 cooperatively transactivate these CRMs. Furthermore, GR and KLF4 or KLF15 occupy viral sequences in these viral CRMs. GC-rich sequences and/or consensus Sp1 family members are essential for transactivation suggesting these transcription factors directly stimulate transcriptional activity. Sp1 and KLF family members belong to the same super-family of transcription factors (63) and interact with GC or CA sequences. Since GR can transactivate promoters when certain GREs are located 5–19 kb pairs from the promoter (64), we cannot rule out that certain GREs participate in activating the expression of these key regulatory viral genes *in vivo*. Finally, one of the HSV-1 origins of replication (oriL) contains a functional GRE, and oriL activity is stimulated by DEX in rat neuronal cells (65). Point mutations in the oriL GRE impair acute infection and reactivation from latency in mice (66). These observations suggest GR activation may have many effects on HSV-1 replication and gene expression.

GR interacts with the p65/p50 heterodimer that binds NF-KB binding sites (67) and represses NF-KB-dependent transcription, which is one reason why GR impairs inflammation and immune responses (29, 68). The immunosuppressive properties of GR and corticosteroids are clearly important for regulating influenza (69) and human cytomegalovirus (70) pathogenesis. A cellular protein, striatin-3, interacts with human GR and forms a trimeric complex with phosphatase 2A, which specifically dephosphorylates serine 211 (71). As expected, dephosphorylation at serine 211 impairs GR-mediated transactivation. Interestingly, GR that is not phosphorylated at serine 211 still exhibits GR-dependent trans-repression. Consequently, the serine 229 GR mutant in GR^{S229A} mice would be expected to control inflammatory responses like wt GR. While we believe GR-mediated transactivation of cellular stress-induced transcription is an early step during successful reactivation from latency, the ability of GR to inhibit inflammation and immune responses will likely promote HSV-1 replication and spread *in vivo*.

MATERIALS AND METHODS

Viruses and cell lines

HSV-1 strain McKrae (NCBI:txid10298, GenBank: OL638991.1) was obtained from the late Dr. Steven Wechsler (University of California, Irvine Medical School) and grown in Vero monkey kidney cells (ATCC CCL-81) that contain minimal essential medium (Corning) supplemented with 10% fetal bovine serum (Atlas Biologicals), 2 mM L-glutamine (Corning), and antibiotics (100 IU/mL penicillin, 100 µg/mL Streptomycin, Cytiva Hyclone) at 37°C, 5% CO2 until >80% CPE (cytopathic effect) was observed. Viral aliquots were obtained through serial freeze-thawing of cells and subsequent centrifugation to remove cellular debris. Virus was titered on Vero cell monolayers to determine PFU/mL for each stock prior to infection of mice.

Mouse breeding and infection studies

The GR^{S229A} mice were developed by Dr. John A. Cidlowski (NIEHS) using targeted embryonic stem (ES) cells in which exon 2 of the mouse *Nr3c1* (GR) gene was replaced with a neomycin cassette flanked by lox71 and lox2272 sites and a recombinase-mediated cassette exchange approach that has been described previously (72). In brief, an exchange vector was generated, which contained exon 2 of the mouse GR gene in which the AGT codon (serine) was mutated to GCT (alanine) at amino acid position 229. The exchange vector also contained a hygromycin selection marker flanked by Frt sites. Flanking the hygromycin and mutant GR S229A exon 2 cassettes were lox66 and lox2272 sites that permit Cre recombinase-dependent directional insertion of DNA in conjunction with the lox71 and lox2272 sites on the targeted allele. The targeted ES cells were transfected with the exchange vector and Cre, and ES cells undergoing successful cassette exchange were confirmed by PCR. The GR^{S229A} positive ES cell clone was injected into C57BL/6J blastocysts (The Jackson Laboratory, 000664) to create chimeric mice. Chimeric males were bred with albino B6(Cg)-*Tyr*$^{c-2J}$/J females (The Jackson Laboratory 000058) to confirm germline transmission, and the hygromycin cassette was deleted by crossing mice with Flp-deleter mice. The resulting $Nr3c1^{S229A/S229A}$ mice (GR^{S229A} knockin) were maintained on a C57BL/6 background. Mice were genotyped by PCR using the following primers: forward, 5′-CTGTTAGAGCATTTCAGTGTGTAGGGACC-3′; reverse, 5′-GGTACTTGCTAACTGAATCCTGAAAATTCTAATC- 3′ giving a fragment size of 230 bp for GR^{S229A} and 180 bp for C57BL/6J(Fig. 1A).

Animals were maintained in Techniplast Blue Line Next individually ventilated cages with 10–15 air changes/h within air-conditioned, temperature and humidity-controlled environments with a 12 h-light/dark cycle. C57BL/6J male and female breeding pairs were purchased from Jackson Labs; GR^{S229A} breeding pairs were developed and gifted by Dr. John A. Cidlowski (NIEHS). All breeders were fed high-fat diet (11% LabDiet, St. Louis, MO, USA) and retained until either 6 months of age or six successful litters (gestational period ~18 days). If dams were found to have dystocia prior to the 6-month timepoint, they were humanely euthanized. GR^{S229A} and wt male and female litter mates were used for each experiment. Pups were sexed and weaned from parental breeding pairs 21 days post-birth and placed in cages (five animals/cage). Between 6 and 8 weeks of age, mice were transferred to disposable Techniplast cages within a BSL-2 approved facility and allowed to acclimate for a minimum of 7 days prior to infection.

All experiments consisted of four to six mice per group with a minimum of two independent experiments. Mice were ocularly infected with 10^5 PFU of HSV-1 strain McKrae without scarification of the eye as previously described (31, 73). Both eyes were infected. Swabs from ocular surfaces were collected every other day for the first 10 dpi followed by swabbing every 5 days for the remainder of the experiment. Plaque assays were performed to measure infectious virus. At 4-, 8-, and 30 dpi, mice were humanely euthanized and tissues were dissected for immunohistochemistry, virus plaquing, or qPCR.

Western blotting

GR^{S229A} and wt mice were treated with vehicle (PBS) or 1 mg of DEX/kg of body weight for 2 h. Lung was collected and lysates were prepared in radio-immunoprecipitation assay (RIPA) buffer with protease and phosphatase inhibitors (cOmplete mini and PhosStop, Roche) and used for western blotting. Samples were quantitated using Bradford assay and ~50 µg protein was loaded on 4–12% Tris-glycine gels (Novex) prior to transferring to LiCor PVDF membrane. Following blocking with 5% non-fat milk in Tris-buffered saline (TBS) with 0.05% Tween-20, membranes were incubated with primary antibody overnight: Phos-Glucocorticoid receptor (Cell Signaling Technology, cat #4161) and total Glucocorticoid receptor D8H2 (Cell Signaling Technology, cat #3660) both 1:1,000 dilution; Actin clone C-4 (Millipore cat# MAB1501) was used as a loading control.

Following primary antibody incubation, membranes were washed and probed with secondary antibody for 1 h at room temperature: Alexa Fluor 680 goat anti-rabbit (Life Technologies) and Goat anti-mouse IRDye 800CW (Licor). Membranes were imaged and quantitated using LiCor Odyssey imaging system.

Primary cell preparation and immunocytochemistry

Kidneys from uninfected GR^{S229A} and wt control animals were aseptically dissected, briefly dipped in 100% ethanol, and immediately stored in MEM + 10% FBS on ice. The capsule of the kidney was manually removed, and the remaining tissue was minced into <3 mm pieces. Kidney pieces were washed three times with PBS and incubated in 0.25% trypsin for 4–18 h at 4°C with rocking. At 4, 8, and 18 h, the supernatant was removed, and single cells were pelleted via centrifugation. Tissue pieces and residual trypsin were moved to 37°C for 30 min and pelleted via centrifugation. Trypsin was removed and an equal volume MEM with L-glutamine, 10% FBS, and antibiotics was added. The remaining tissue and cells were gently dispersed by pipetting, filtered through a 100 µm cell strainer, and viability was determined via trypan blue assay.

Approximately 48 h post-isolation, cells were plated onto 8-well chamber slides (NUNC Lab Tek II, Cat #: 154534) and grown for 24–48 h. Media was replaced with MEM containing 2% charcoal-stripped FBS (Sigma) and 10 µM water-soluble DEX (Sigma) for 4 h prior to fixation using 100% chilled methanol for 5 min. Samples without DEX were included as controls. Cells were washed with TBS and incubated with either total GR (Cell Signaling Technology, 1:2,000 dilution) or phos-GR antibody (Cell Signaling Technology, 1:1,600 dilution) overnight at 4°C. Antibodies directed against HSV-1 viral proteins are: anti-ICP0 antibody (Santa Cruz Biotechnology, sc-53070) that was diluted 1:50, anti-ICP4 antibody (Abcam, ab6514) that was diluted 1:250, and anti-VP16 antibody (Abcam, ab110226) that was diluted 1:100. The next day, cells were washed with TBS and incubated with secondary Alexa fluor 488 (Invitrogen) for 1 h at room temperature in the dark. Cells were washed with TBS and stained with 4′,6-diamidino-2-phenylindole, dihydrochloride (DAPI, ThermoFisher Scientific) for 10 min at room temperature prior to mounting of coverslips. Images were obtained with an Olympus BX microscope and CellSense Entry software with exposure times of ~50 (DAPI) and ~400 milliseconds (Alexa).

Infection of primary mouse kidney cells

Following isolation, primary mouse kidney cells were counted and plated in 24-well plates prior to infection with HSV-1 at a multiplicity of infection of 1 at 37°C, 5% CO2 with rocking. Virus was removed and cells were incubated for 24 h prior to plaquing for virus titers on Vero cells as described above. Data are shown as mean ± SD for PFU/mL × 10^3. $^{**}P < 0.01$ and $^{***}P < 0.005$ by Student's *t*-test. NS, not significant.

Ocular swabs, TG plaquing, and explant-induced reactivation

For each timepoint, swabs from ocular surfaces were collected from individual animals in 1 mL MEM with L-glutamine, antibiotics, and 10% FBS. Samples were frozen until ready

for use. Serial dilutions of ocular swabs were used to infect Vero monolayers for 1 h at 37°C, 5% CO_2 with rocking. Monolayers were overlayed with 1% methylcellulose in MEM with L-glutamine, 10% FBS, and antibiotics and monitored for visible plaques. If no plaques were observed after 72 h, samples were considered negative for the virus.

At 4- and 8 days post-infection, TG were isolated, minced into three to four pieces, and placed in 60 mm dishes with confluent Vero monolayers. If CPE was detected within 24 h (4 dpi), cells and supernatant were collected, serially frozen/thawed (−80 to 37°C), and titered on Vero monolayers. If no CPE was observed (8 dpi), tissue and supernatant were removed and 1% methylcellulose in MEM with L-glutamine, 10% FBS, and antibiotics was overlayed onto the monolayer and allowed to incubate for 3 days prior to crystal violet staining for plaque visualization.

For explant-induced reactivation, TG were collected 30 dpi in MEM with L-glutamine, antibiotics, 2% charcoal-stripped FBS, and 10 µM DEX. Aliquots of supernatant were removed daily for 10 days and used to plaque for infectious virus on Vero monolayers.

Reverse transcription and quantitative polymerase chain reaction

TG and kidney were dissected and processed as previously described with modifications for qPCR (74). Kidneys were used as internal negative reference tissues as they do not contain any HSV-1 DNA following ocular infection. The use of an internal reference tissue within the same animal as experimental samples provides a twofold reduction in technical variation and PCR efficiency (75).

Tissues were incubated in 25 mM NaOH at 99°C for 1 h and homogenized using a sterile, disposable microtube pestle. An equal volume of 40 mM Tris-HCl (pH 5.5) was added to neutralize the NaOH. Tubes were briefly centrifuged to pellet debris and supernatant was used for ethanol precipitation. Roughly two volumes of ice-cold ethanol were added to the supernatant and incubated at −20°C overnight. DNA was pelleted via centrifugation (18,000 *g* for 30 min), washed twice with 70% ethanol, and air-dried prior to dissolving in diethyl dicarbonate (DEPC)-water. A total of 100 ng of DNA was used as a template for Sybr Green qPCR (Applied Biosciences) using primers for HSV-1 gB and mouse GAPDH. gB forward primer 5′- AACGCGACGCACATCAAG; gB reverse primer 5′- CTGGTACGCGATCAGAAAGC; GAPDH forward primer 5′- CATCACTGCCACCCAGAAGACTG; GAPDH reverse primer 5′- ATGCCAGTGAGCTTCCCGTTCAG.

For RT-qPCR, 30 dpi TG and kidney were dissected and homogenized in Trizol using GentleMACS M-tubes and program RNA_01. M Tubes were centrifuged at 2,000 *g* for 5 min prior to application with the Qiagen RNeasy Kit according to the manufacturer's instructions. Samples were eluted with DEPC-water and analyzed for yield and quality using an agarose gel. If DNA was present, samples were treated with DNAseI turbo (Thermo) at 37°C for 10 min prior to re-purification using the RNeasy kit. Samples were stored at −80°C until use. cDNA synthesis was performed using SuperScript II Reverse Transcriptase (RT, Invitrogen) according to the manufacturer's instructions. Briefly, ~1 µg RNA was combined with random hexamers (250 ng/µL) and dNTPs (10 mM) and incubated at 65°C for 5 min prior to chilling. RNAseOUT and DTT were added for 2 min at 25°C followed by RT added at 25°C for 10 min. The entire reaction mixture was then incubated at 50°C for 1 h followed by enzyme inactivation at 85°C for 5 min. cDNA was quantified via nanodrop and used for qPCR as described above substituting primers for HSV-1 LAT and mouse GAPDH. LAT forward primer 5′- CCTTATCTAAGGGCCGGCTG; LAT rev primer 5′- GGGACACATGCCTTCTTGGA.

All primers were designed through IDT. BioRad CFX Opus 96 PCR system was used along with CFX Maestro Analysis Software: Cq values between 20 and 35 were considered positive. Ratios of gB or LAT to GAPDH were calculated using the Delta-Delta CT method.

Immunohistochemistry

TG from infected animals were harvested and placed directly into neutral buffered formalin. Preparation of slides and subsequent IHC were performed as described (75, 76).

Thin sections of paraffin-embedded TG (4–5 µm) were mounted onto positively charged glass slides and air-dried a minimum of 24 h prior to staining. Slides were heated at 65°C for 30 min and deparaffinized in xylene. Serial rehydration followed using decreasing concentrations of ethanol. Endogenous peroxidases were blocked using 0.045% hydrogen peroxide for 30 min at room temperature in the dark. Antigen retrieval was performed using proteinase K (Dako) at 37°C for 30 min followed by blocking the slides with animal-free blocking solution (AFBS, Cell Signaling Technology) for a minimum of 45 min at room temp. Vector Labs avidin/biotin blocking kit was used according to the manufacturer's instructions. Primary antibodies were diluted in AFBS (1:200 phos-GR; 1:500 GR, 1:100 ICP0 and VP16, 1:200 ICP4) and slides were incubated overnight at 4°C. The following day, biotinylated secondary antibody from the Vectastain ABC kit, diluted in AFBS, was applied for 30 min at room temperature. NovaRED substrate (Vector labs) was used for color development followed by counterstaining with Mayer's hematoxylin.

All slides were imaged using an Olympus BX43 microscope and CellSense Entry software with auto exposure and processed using Fiji (ImageJ) (76). A minimum of 500 neurons were counted and data were calculated as % positive = ratio of positive neurons to total neurons per field of view.

Statistical analysis

All graphs and comparisons were performed using GraphPad Prism software (v9.5.1). *P* values less than 0.05 were considered significant for all calculations.

ACKNOWLEDGMENTS

We thank Dr. Amy J. Galliher-Beckley of the Signal Transduction Laboratory (NIEHS) and Dr. Manas K. Ray of the Knockout Mouse Core Facility (NIEHS) for their assistance in generating the GR^{S229A} knockin mice. Finally, we thank Abigael Anderson and Susan Muench of Oklahoma State University Lab Animal Resources for their assistance with animal husbandry and breeding.

This research was supported by grants to C.J. from the National Institute of Neurological Disorders and Stroke (R01NS111167), funds from the Oklahoma Center for Respiratory and Infectious Diseases (National Institutes of Health Centers for Biomedical Research Excellence Grant # P20GM103648), and funds from the Sitlington Endowment. The OSU CVM RAC seed grant program also supported these studies (K.S.H.). This research was also supported by the Intramural Research Program of the NIH, NIEHS (ZIAES090057, J.A.C.).

The authors have declared that no conflict of interest exists.

AUTHOR AFFILIATIONS

[1]Department of Veterinary Pathobiology, College of Veterinary Medicine, Oklahoma State University, Stillwater, Oklahoma, USA
[2]National Institute of Environmental Health Sciences, National Institutes of Health, Research Triangle Park, North Carolina, USA

AUTHOR ORCIDs

Vanessa C. Santos http://orcid.org/0000-0001-9048-7999
Clinton Jones http://orcid.org/0000-0002-6656-4971

FUNDING

Funder	Grant(s)	Author(s)
HHS | NIH | National Institute of Neurological Disorders and Stroke (NINDS)	R01NS111167	Clinton Jones

Funder	Grant(s)	Author(s)
HHS | NIH | NIH Office of the Director (OD)	P20GM103648	Clinton Jones
HHS | NIH | National Institute of Environmental Health Sciences (NIEHS)	ZIAES090057	John A. Cidlowski

AUTHOR CONTRIBUTIONS

Kelly S. Harrison, Conceptualization, Data curation, Funding acquisition, Investigation, Methodology, Project administration, Software, Supervision, Validation, Visualization, Writing – original draft, Writing – review and editing | Nishani Wijesekera, Conceptualization, Data curation, Funding acquisition, Investigation, Methodology, Project administration, Resources, Software, Supervision, Validation, Visualization, Writing – original draft, Writing – review and editing | Anastasia G. J. Robinson, Formal analysis, Investigation, Methodology, Visualization, Writing – review and editing | Vanessa C. Santos, Formal analysis, Validation, Writing – review and editing | Robert H. Oakley, Conceptualization, Formal analysis, Methodology, Resources, Writing – review and editing | John A. Cidlowski, Conceptualization, Data curation, Funding acquisition, Methodology, Project administration, Resources, Software, Validation, Writing – review and editing | Clinton Jones, Conceptualization, Data curation, Funding acquisition, Investigation, Methodology, Project administration, Resources, Software, Supervision, Validation, Visualization, Writing – original draft, Writing – review and editing

ETHICS APPROVAL

All animal experiments were approved and performed according to the guidelines of the respective institution in which they were performed. Generation of GR^{S229A} knocking mice was performed at NIEHS under Animal Care and Use Committee (protocol 2008–0021). HSV-1 infection and subsequent experiments were performed in accordance with the Oklahoma State University Institutional Animal Care and Use Committee, protocol VM-21-–86.

REFERENCES

1. Fraser NW, Lawrence WC, Wroblewska Z, Gilden DH, Koprowski H. 1981. Herpes simplex virus type 1 DNA in human brain tissue. Proc Natl Acad Sci U S A 78:6461–6465. https://doi.org/10.1073/pnas.78.10.6461
2. Cabrera CV, Wohlenberg C, Openshaw H, Rey-Mendez M, Puga A, Notkins AL. 1980. Herpes simplex virus DNA sequences in the CNS of latently infected mice. Nature 288:288–290. https://doi.org/10.1038/288288a0
3. Rock DL, Fraser NW. 1983. Detection of HSV-1 genome in central nervous system of latently infected mice. Nature 302:523–525. https://doi.org/10.1038/302523a0
4. Smith RE, McDonald HR, Nesburn AB, Minckler DS. 1980. Penetrating keratoplasty: changing indications, 1947 to 1978. Arch Ophthalmol 98:1226–1229. https://doi.org/10.1001/archopht.1980.01020040078009
5. Pavan-Langston D. 2000. Herpes simplex of the ocular anterior segment. Curr Clin Top Infect Dis 20:298–324.
6. Wilhelmus KR, Beck RW, Moke PS, Dawson CR, Barron BA, Jones DB, Kaufman HE, Kurinij N, Stulting RD, Sugar J, Cohen EJ, Hyndiuk RA, Asbell PA. 1998. Acyclovir for the prevention of recurrent herpes simplex virus eye disease. N Engl J Med 339:300–306. https://doi.org/10.1056/NEJM199807303390503
7. Shimeld C, Efstathiou S, Hill T. 2001. Tracking the spread of a lacZ-tagged herpes simplex virus type 1 between the eye and the nervous system of the mouse: comparison of primary and recurrent infection. J Virol 75:5252–5262. https://doi.org/10.1128/JVI.75.11.5252-5262.2001
8. Skoldenberg B. 1991. Herpes Simplex encephalitis. Scand J Infect Dis Suppl 80:40–46. https://doi.org/10.1007/s40588-023-00202-9
9. Stahl JP, Mailles A, Dacheux L, Morand P. 2011. Epidemiology of viral encephalitis in 2011. Med Mal Infect 41:453–464. https://doi.org/10.1016/j.medmal.2011.05.015
10. Yamada S, Kameyama T, Nagaya S, Hashizume Y, Yoshida M. 2003. Relapsing herpes simplex encephalitis: pathological confirmation of viral reactivation. J Neurol Neurosurg Psychiatry 74:262–264. https://doi.org/10.1136/jnnp.74.2.262
11. Rantalaiho T, Färkkilä M, Vaheri A, Koskiniemi M. 2001. Acute encephalitis from 1967 to 1991. J Neurol Sci 184:169–177. https://doi.org/10.1016/s0022-510x(01)00441-5
12. Jones C. 2023. Intimate relationship between stress and human alphaherpes virus (HSV-1) reactivation from latency. Curr Clin Micro Rpt. https://doi.org/10.1007/s40588-023-00202-9
13. Jones C. 1998. Alphaherpesvirus latency: its role in disease and survival of the virus in nature. Adv Virus Res 51:81–133. https://doi.org/10.1016/s0065-3527(08)60784-8
14. Perng G-C, Jones C. 2010. Towards an understanding of the herpes simplex virus type 1 latency-reactivation cycle. Interdiscip Perspect Infect Dis 2010:262415. https://doi.org/10.1155/2010/262415
15. Phelan D, Barrozo ER, Bloom DC. 2017. HSV1 latent transcription and non-coding RNA: a critical retrospective. J Neuroimmunol 308:65–101. https://doi.org/10.1016/j.jneuroim.2017.03.002
16. Thompson RL, Sawtell NM. 1997. The herpes simplex virus type 1 latency-associated transcript gene regulates the establishment of latency. J Virol 71:5432–5440. https://doi.org/10.1128/JVI.71.7.5432-5440.1997
17. Umbach JL, Kramer MF, Jurak I, Karnowski HW, Coen DM, Cullen BR. 2008. MicroRNAs expressed by herpes simplex virus 1 during latent infection regulate viral mRNAs. Nature 454:780–783. https://doi.org/10.1038/nature07103
18. Umbach JL, Nagel MA, Cohrs RJ, Gilden DH, Cullen BR. 2009. Analysis of human alphaherpesvirus microRNA expression in latently infected

human trigeminal ganglia. J Virol 83:10677–10683. https://doi.org/10.1128/JVI.01185-09
19. Du T, Zhou G, Roizman B. 2011. HSV-1 gene expression from reactivated ganglia is disordered and concurrent with suppression of latency-associated transcript and miRNAs. Proc Natl Acad Sci U S A 108:18820–18824. https://doi.org/10.1073/pnas.1117203108
20. Perng G-C, Maguen B, Jin L, Mott KR, Kurylo J, BenMohamed L, Yukht A, Osorio N, Nesburn AB, Henderson G, Inman M, Jones C, Wechsler SL. 2002. A novel herpes simplex virus type 1 transcript (AL-RNA) antisense to the 5′ end of the latency-associated transcript produces a protein in infected rabbits. J Virol 76:8003–8010. https://doi.org/10.1128/jvi.76.16.8003-8010.2002
21. Thompson RL, Sawtell NM. 2011. The herpes simplex virus type 1 latency associated transcript locus is required for the maintenance of reactivation competent latent infections. J Neurovirol 17:552–558. https://doi.org/10.1007/s13365-011-0071-0
22. Ahmed M, Lock M, Miller CG, Fraser NW. 2002. Regions of the herpes simplex virus type 1 latency-associated transcript that protect cells from apoptosis in vitro and protect neuronal cells *in vivo*. J Virol 76:717–729. https://doi.org/10.1128/jvi.76.2.717-729.2002
23. Branco FJ, Fraser NW. 2005. Herpes simplex virus type 1 latency-associated transcript expression protects trigeminal ganglion neurons from apoptosis. J Virol 79:9019–9025. https://doi.org/10.1128/JVI.79.14.9019-9025.2005
24. Carpenter D, Hsiang C, Brown DJ, Jin L, Osorio N, BenMohamed L, Jones C, Wechsler SL. 2007. Stable cell lines expressing high levels of the herpes simplex virus type 1 LAT are refractory to caspase 3 activation and DNA laddering following cold shock induced apoptosis. Virology 369:12–18. https://doi.org/10.1016/j.virol.2007.07.023
25. Shen W, Sa e Silva M, Jaber T, Vitvitskaia O, Li S, Henderson G, Jones C. 2009. Two small RNAs encoded within the first 1.5 kilobases of the herpes simplex virus type 1 latency-associated transcript can inhibit productive infection and cooperate to inhibit apoptosis. J Virol 83:9131–9139. https://doi.org/10.1128/JVI.00871-09
26. Glaser R, Kiecolt-Glaser JK, Speicher CE, Holliday JE. 1985. Stress, loneliness, and changes in herpesvirus latency. J Behav Med 8:249–260. https://doi.org/10.1007/BF00870312
27. Glaser R, Kiecolt-Glaser JK. 2005. Stress-induced immune dysfunction: implications for health. Nat Rev Immunol 5:243–251. https://doi.org/10.1038/nri1571
28. Padgett DA, Sheridan JF, Dorne J, Berntson GG, Candelora J, Glaser R. 1998. Social stress and the reactivation of latent herpes simplex virus type 1. Proc Natl Acad Sci U S A 95:7231–7235. https://doi.org/10.1073/pnas.95.12.7231
29. Smoak KA, Cidlowski JA. 2004. Mechanisms of glucocorticoid receptor signaling during inflammation. Mech Ageing Dev 125:697–706. https://doi.org/10.1016/j.mad.2004.06.010
30. Oakley RH, Cidlowski JA. 2013. The biology of the glucocorticoid receptor: New signaling mechanisms in health and disease. J Allergy Clin Immunol 132:1033–1044. https://doi.org/10.1016/j.jaci.2013.09.007
31. Harrison KS, Zhu L, Thunuguntla P, Jones C. 2019. Antagonizing the glucocorticoid receptor impairs explant-induced reactivation in mice latently infected with herpes simplex virus 1. J Virol 93:e00418-19. https://doi.org/10.1128/JVI.00418-19
32. DeLeón M, Coveñas R, Chadi G, Narváez JA, Fuxe K, Cintra A. 1994. Subpopulations of primary sensory neurons show coexistence of neuropeptides and glucocorticoid receptors in the rat spinal and trigeminal ganglia. Brain Res 636:338–342. https://doi.org/10.1016/0006-8993(94)91034-0
33. Ostler JB, Harrison KS, Schroeder K, Thunuguntla P, Jones C. 2019. The glucocorticoid receptor (GR) stimulates herpes simplex virus 1 productive infection, in part because the infected cell protein 0 (ICP0) promoter is cooperatively transactivated by the GR and Krüppel-like transcription factor 15. J Virol 93:e02063-18. https://doi.org/10.1128/JVI.02063-18
34. Wijesekera N, Hazell N, Jones C. 2022. Independent cis-regulatory modules within the herpes simplex virus 1 infected cell protein 0 (ICP0) promoter are transactivated by Krüppel-like factor 15 and glucocorticoid receptor. Viruses 14:1284. https://doi.org/10.3390/v14061284
35. Ostler JB, Thunuguntla P, Hendrickson BY, Jones C. 2021. Transactivation of herpes simplex virus 1 (HSV-1) infected cell protein 4 enhancer by glucocorticoid receptor and stress-induced transcription factors requires overlapping Krüppel-like transcription factor 4/SP1 binding sites. J Virol 95:e01776-20. https://doi.org/10.1128/JVI.01776-20
36. Ostler JB, Jones C. 2021. Stress induced transcription factors transactivate the herpes simplex virus 1 infected cell protein 27 (ICP27) transcriptional enhancer. Viruses 13:2296. https://doi.org/10.3390/v13112296
37. Santos VC, Ostler JB, Harrison KS, Jones C. 2023. Slug, a stress-induced transcription factor, stimulates herpes simplex virus 1 replication and transactivates a *cis*-regulatory module within the VP16 promoter. J Virol 97:e0007323. https://doi.org/10.1128/jvi.00073-23
38. Rhen T, Cidlowski JA. 2005. Anti-inflammatory action of glucocorticoids - new mechanisms of old drugs. N Engl J Med 353:1711–1723. https://doi.org/10.1056/NEJMra050541
39. Galliher-Beckley AJ, Cidlowski JA. 2009. Emerging roles of glucocorticoid receptor phosphorylation in modulating glucocorticoid hormone action in health and disease. IUBMB Life 61:979–986. https://doi.org/10.1002/iub.245
40. Khan SH, McLaughlin WA, Kumar R. 2017. Site-specific phosphorylation regulates the structure and function of an intrinsically disordered domain of the glucocorticoid receptor. Sci Rep 7:15440. https://doi.org/10.1038/s41598-017-15549-5
41. Cole TJ, Blendy JA, Monaghan AP, Krieglstein K, Schmid W, Aguzzi A, Fantuzzi G, Hummler E, Unsicker K, Schütz G. 1995. Targeted disruption of the glucocorticoid receptor gene blocks adrenergic chromaffin cell development and severely retards lung maturation. Genes Dev 9:1608–1621. https://doi.org/10.1101/gad.9.13.1608
42. Oitzl MS, de Kloet ER, Joëls M, Schmid W, Cole TJ. 1997. Spatial learning deficits in mice with a targeted glucocorticoid receptor gene disruption. Eur J Neurosci 9:2284–2296. https://doi.org/10.1111/j.1460-9568.1997.tb01646.x
43. Tronche F, Kellendonk C, Kretz O, Gass P, Anlag K, Orban PC, Bock R, Klein R, Schütz G. 1999. Disruption of the glucocorticoid receptor gene in the nervous system results in reduced anxiety. Nat Genet 23:99–103. https://doi.org/10.1038/12703
44. Kellendonk C, Eiden S, Kretz O, Schütz G, Schmidt I, Tronche F, Simon E. 2002. Inactivation of the GR in the nervous system affects energy accumulation. Endocrinology 143:2333–2340. https://doi.org/10.1210/endo.143.6.8853
45. Chen W, Dang T, Blind RD, Wang Z, Cavasotto CN, Hittelman AB, Rogatsky I, Logan SK, Garabedian MJ. 2008. Glucocorticoid receptor phosphorylation differentially affects target gene expression. Mol Endocrinol 22:1754–1766. https://doi.org/10.1210/me.2007-0219
46. Lewandowski G, Zimmerman MN, Denk LL, Porter DD, Prince GA. 2002. Herpes simplex type 1 infects and establishes latency in the brain and trigeminal ganglia during primary infection of the lip in cotton rats and mice. Arch Virol 147:167–179. https://doi.org/10.1007/s705-002-8309-9
47. Cai WH, Gu B, Person S. 1988. Role of glycoprotein B of herpes simplex virus type 1 in viral entry and cell fusion. J Virol 62:2596–2604. https://doi.org/10.1128/JVI.62.8.2596-2604.1988
48. Agelidis AM, Shukla D. 2015. Cell entry mechanisms of HSV: What we have learned in recent years. Future Virol 10:1145–1154. https://doi.org/10.2217/fvl.15.85
49. Pataki Z, Sanders EK, Heldwein EE. 2022. A surface pocket in the cytoplasmic domain of the herpes simplex virus fusogen gB controls membrane fusion. PLoS Pathog 18:e1010435. https://doi.org/10.1371/journal.ppat.1010435
50. Doll JR, Sawtell NM, Sandri-Goldin RM. 2017. Analysis of herpes simplex virus reactivation in explant reveals a method-dependent difference in measured timing of reactivation. J Virol 91:00848–17. https://doi.org/10.1128/JVI.00848-17
51. Cassidy L, Meadows J, Catalán J, Barton S. 1997. Are stress and coping style associated with frequent recurrence of genital herpes Genitourin Med 73:263–266. https://doi.org/10.1136/sti.73.4.263
52. Rooney JF, Straus SE, Mannix ML, Wohlenberg CR, Banks S, Jagannath S, Brauer JE, Notkins AL. 1992. UV light-induced reactivation of herpes simplex virus type 2 and prevention by acyclovir. J Infect Dis 166:500–506. https://doi.org/10.1093/infdis/166.3.500
53. Noisakran S, Halford WP, Veress L, Carr DJJ. 1998. Role of the hypothalamic pituitary adrenal axis and IL-6 in stress-induced reactivation of latent

herpes simplex virus type 1. J Immunol 160:5441–5447. https://doi.org/10.4049/jimmunol.160.11.5441
54. Du T, Zhou G, Roizman B. 2012. Induction of apoptosis accelerates reactivation from latent HSV-1 in ganglionic organ cultures and replication in cell cultures. Proc Natl Acad Sci U S A 109:14616–14621. https://doi.org/10.1073/pnas.1212661109
55. Skobowiat C, Sayre RM, Dowdy JC, Slominski AT. 2013. Ultraviolet radiation regulates cortisol activity in a waveband-dependent manner in human skin ex vivo. Br J Dermatol 168:595–601. https://doi.org/10.1111/bjd.12096
56. Skobowiat C, Postlethwaite AE, Slominski AT. 2017. Skin exposure to ultraviolet B rapidly activates systemic neuroendocrine and immunosuppressive responses. Photochem Photobiol 93:1008–1015. https://doi.org/10.1111/php.12642
57. Suzich JB, Cliffe AR. 2018. Strength in diversity: understanding the pathways to herpes simplex virus reactivation. Virology 522:81–91. https://doi.org/10.1016/j.virol.2018.07.011
58. Wilson AC. 2022. Impact of cultured neuron models on A-Herpesvirus latency research. Viruses 14:1209. https://doi.org/10.3390/v14061209
59. Arancibia S, Benítez D, Núñez LE, Jewell CM, Langjahr P, Candia E, Zapata-Torres G, Cidlowski JA, González M-J, Hermoso MA. 2011. Phosphatidylinositol 3-kinase interacts with the glucocorticoid receptor upon TLR2 activation. J Cell Mol Med 15:339–349. https://doi.org/10.1111/j.1582-4934.2009.00958.x
60. Wang X, Hu J, Price SR. 2007. Inhibition of PI3-kinase signaling by glucocorticoids results in increased branched-chain amino acid degradation in renal epithelial cells. Am J Physiol Cell Physiol 292:C1874–C1879. https://doi.org/10.1152/ajpcell.00617.2006
61. Mecklenburg J, Zou Y, Wangzhou A, Garcia D, Lai Z, Tumanov AV, Dussor G, Price TJ, Akopian AN. 2020. Transcriptomic sex differences in sensory neuronal populations of mice. Sci Rep 10:15278. https://doi.org/10.1038/s41598-020-72285-z
62. Spaanderman DCE, Nixon M, Buurstede JC, Sips HC, Schilperoort M, Kuipers EN, Backer EA, Kooijman S, Rensen PCN, Homer NZM, Walker BR, Meijer OC, Kroon J. 2018. Androgens modulate glucocorticoid receptor activity in adipose tissue and liver. J Endocrinol, October:JOE-18-0503.R1. https://doi.org/10.1530/JOE-18-0503
63. Black AR, Black JD, Azizkhan-Clifford J. 2001. Sp1 and Krüppel-like factor family of transcription factors in cell growth regulation and cancer. J Cell Physiol 188:143–160. https://doi.org/10.1002/jcp.1111
64. Polman JAE, Welten JE, Bosch DS, de Jonge RT, Balog J, van der Maarel SM, de Kloet ER, Datson NA. 2012. A genome-wide signature of glucocorticoid receptor binding in neuronal PC12 cells. BMC Neurosci 13:118. https://doi.org/10.1186/1471-2202-13-118
65. Hardwicke MA, Schaffer PA. 1997. Differential effects of nerve growth factor and dexamethasone on herpes simplex virus type 1 oriL- and oriS-dependent DNA replication in PC12 cells. J Virol 71:3580–3587. https://doi.org/10.1128/JVI.71.5.3580-3587.1997
66. Balliet JW, Schaffer PA. 2006. Point mutations in herpes simplex virus type 1 oriL, but not in oriS, reduce pathogenesis during acute infection of mice and impair reactivation from latency. J Virol 80:440–450. https://doi.org/10.1128/JVI.80.1.440-450.2006
67. Oeckinghaus A, Ghosh S. 2009. The NF-kappaB family of transcription factors and its regulation. Cold Spring Harb Perspect Biol 1:a000034. https://doi.org/10.1101/cshperspect.a000034
68. Cain DW, Cidlowski JA. 2017. Immune regulation by glucocorticoids. Nat Rev Immunol 17:233–247. https://doi.org/10.1038/nri.2017.1
69. Jamieson AM, Yu S, Annicelli CH, Medzhitov R. 2010. Influenza virus-induced glucocorticoids compromise innate host defense against a secondary bacterial infection. Cell Host Microbe 7:103–114. https://doi.org/10.1016/j.chom.2010.01.010
70. Quatrini L, Wieduwild E, Escaliere B, Filtjens J, Chasson L, Laprie C, Vivier E, Ugolini S. 2018. Endogenous glucocorticoids control host resistance to viral infection through the tissue-specific regulation of PD-1 expression on NK cells. Nat Immunol 19:954–962. https://doi.org/10.1038/s41590-018-0185-0
71. Petta I, Bougarne N, Vandewalle J, Dejager L, Vandevyver S, Ballegeer M, Desmet S, Thommis J, De Cauwer L, Lievens S, Libert C, Tavernier J, De Bosscher K. 2017. Glucocorticoid receptor-mediated transactivation is hampered by striatin-3, a novel interaction partner of the receptor. Sci Rep 7:8941. https://doi.org/10.1038/s41598-017-09246-6
72. Oakley RH, Ramamoorthy S, Foley JF, Busada JT, Lu NZ, Cidlowski JA. 2018. Glucocorticoid receptor Isoform-specific regulation of development, circadian rhythm, and inflammation in mice. FASEB J 32:5258–5271. https://doi.org/10.1096/fj.201701153R
73. Harrison KS, Zhu L, Thunuguntla P, Jones C. 2020. Herpes simplex virus 1 regulates β-catenin expression in TG neurons during the latency-reactivation cycle. PLoS One 15:e0230870. https://doi.org/10.1371/journal.pone.0230870
74. Truett GE, Heeger P, Mynatt RL, Truett AA, Walker JA, Warman ML. 2000. Preparation of PCR-quality mouse genomic DNA with hot sodium hydroxide and tris (HotSHOT). Biotechniques 29:52, 54. https://doi.org/10.2144/00291bm09
75. Workman A, Zhu L, Keel BN, Smith TPL, Jones C, Longnecker RM. 2018. The Wnt signaling pathway is differentially expressed during the bovine herpesvirus 1 latency-reactivation cycle: evidence that two protein kinases associated with neuronal survival, Akt3 and BMPR2, are expressed at higher levels during latency. J Virol 92:e01937-17. https://doi.org/10.1128/JVI.01937-17
76. Schindelin J, Arganda-Carreras I, Frise E, Kaynig V, Longair M, Pietzsch T, Preibisch S, Rueden C, Saalfeld S, Schmid B, Tinevez J-Y, White DJ, Hartenstein V, Eliceiri K, Tomancak P, Cardona A. 2012. Fiji: an open-source platform for biological-image analysis. Nat Methods 9:676–682. https://doi.org/10.1038/nmeth.2019